



OPEN ACCESS

EDITED BY

Salah Kamel,
Aswan University, Egypt

REVIEWED BY

Saad Mekhilef,
Swinburne University of Technology,
Australia
Yashwant Sawle,
Madhav Institute of Technology and
Science Gwalior, India

*CORRESPONDENCE

Ruhi Sharmin,
rsharmin@purdue.edu

SPECIALTY SECTION

This article was submitted to Solar
Energy,
a section of the journal
Frontiers in Energy Research

RECEIVED 30 April 2022

ACCEPTED 04 July 2022

PUBLISHED 30 August 2022

CITATION

Sharmin R, Chowdhury SS, Abedin F and
Rahman KM (2022), Implementation of
an MPPT technique of a solar module
with supervised machine learning.
Front. Energy Res. 10:932653.
doi: 10.3389/fenrg.2022.932653

COPYRIGHT

© 2022 Sharmin, Chowdhury, Abedin
and Rahman. This is an open-access
article distributed under the terms of the
[Creative Commons Attribution License
\(CC BY\)](https://creativecommons.org/licenses/by/4.0/). The use, distribution or
reproduction in other forums is
permitted, provided the original
author(s) and the copyright owner(s) are
credited and that the original
publication in this journal is cited, in
accordance with accepted academic
practice. No use, distribution or
reproduction is permitted which does
not comply with these terms.

Implementation of an MPPT technique of a solar module with supervised machine learning

Ruhi Sharmin*, Sayeed Shafayet Chowdhury, Farihal Abedin and Kazi Mujibur Rahman

Department of Electrical and Electronic Engineering (EEE) of Bangladesh University of Engineering and Technology (BUET), Dhaka, Bangladesh

Automated calibration of a maximum power point tracking (MPPT) algorithm for the photovoltaic (PV) system is pivotal for harnessing the maximum possible energy from solar power. However, most existing calibration methods of such an MPPT system are cumbersome and vary greatly with the environmental condition. Hence, an automated pipeline capable of performing suitable adjustments is highly desirable. We proposed a method using supervised machine learning (ML) in a solar PV system for MPPT analysis. For this purpose, an overall schematic diagram of a PV system is designed and simulated to create a dataset in MATLAB/Simulink. Thus, by analyzing the output characteristics of a solar cell, an improved MPPT algorithm on the basis of a neural network (NN) method is put forward to track the maximum power point (MPP) of solar cell modules. Moreover, we implemented the algorithm in a hardware setup and verified the theoretical result with the empirical data. Typically, the performance accuracy of the NN models is around 97~98%. But our proposed model shows an even higher efficiency (99.8% approximately) without adding to any extra computational cost.

KEYWORDS

MPPT, solar, MATLAB/Simulink ©, machine learning, PV panel

1 Introduction

With the advent of modern technology, renewable energy is the most talked about topic in the world nowadays, mostly because of the global energy crisis. Consequently, the search for green energy has led us to various forms of renewable energy, which derive directly from the Sun or from heat generated deep within Earth. Included in the definition is electricity and heat generated from solar, wind, ocean, hydropower, biomass, geothermal resources, and bio-fuels and hydrogen derived from renewable resources. Among them, solar energy is abundant in nature and does not pose any threat to environmental hazards, and hence, is the safest option as a reliable power source (Ramirez-Del-Barrio, 2017). Engineers developing solar inverters implement maximum power point tracking (MPPT) algorithms to maximize the power generated by photovoltaic (PV) solar systems (Mayatake et al., 2011). The algorithms account for factors such as variable irradiance (sunlight) and temperature to ensure that the PV

system generates maximum power at all times, making MPPT a crucial factor (Hohm and Ropp, 2002; ESRAM and Chapman, 2007; de Brito et al., 2013; Motahhir et al., 2020). There are several algorithms for MPPT analysis but each of them can be categorized based on the type of the control variable it uses: 1) voltage; 2) current; or 3) duty cycle. The main advantage of these algorithms is their capability and flexibility to solve non-linear problems. Moreover, they can generate the optimal solution or multi-peak MPPT for global maxima with acceptable efficiency. So, these methods show superior tracking performance over conventional algorithms (Rezk and Eltamaly, 2015) (Subudhi and Pradhan, 2013). To track the maximum power point (MPP) efficiently, numerous algorithms have been proposed so far, such as the perturb and observe (P&O) method, incremental conductance (IC) method, fractional open-circuit voltage (FOCV) method, short circuit current method, fuzzy logic-based algorithm etc. While these approaches perform well and produce overall acceptable results, the recent surge of data-driven machine learning (ML) approaches holds great promise in this research domain. Since supervised ML methods are trained directly based on the data, no human-designed heuristics are involved, which makes these techniques highly accurate and robust.

Discussing previous works on MPPT algorithms first leads to the perturb and observe (P&O) method which is very simple and basic yet unacceptable in many cases because of its lesser accuracy (Ibrahim et al., 2015) (Azad et al., 2017). For example, in a real-life set-up, it is assumed that the system does oscillate around the MPP, indicating that a continuous perturbation in one fixed direction will lead to an operating point which will be very far away from the actual MPP. This process continues until the increase in insolation is reduced or eliminated completely. Among other existing methods, the incremental conductance (IC) method comes immediately after the P&O method (Barua et al., 2016). Despite its higher accuracy in comparison with the P&O method, it is not so easy to implement. Both perturb and observe and the incremental conductance are ideal examples of “hill climbing” algorithms that can find the local maximum power point of the power curve for the operating condition of the solar PV array. However, the fractional open circuit voltage method and fractional short circuit current method are also popular because of their improved efficiency than that of the P&O method (Frezza et al., 2014). Fuzzy logic is a bit complicated to implement but gives satisfying results (Chekired et al., 2011) (Li and Wang, 2009). Also, fuzzy logic can reduce the slower tracking speed and the oscillation noise around the maximum power point (MPP) which are the two main disadvantages of the P&O method. But in this era of artificial intelligence and the boom of neural network architecture, using machine learning gives the most accurate results within the shortest possible time span. As a result, no other MPPT algorithm can beat the level of efficiency provided by a neural network model of the solar MPPT controller. This

study supports this claim. Therefore, from the literature search, it is evident that using ML-based models will not only increase the performance accuracy but also automate the maximum power point tracking process.

In this study, an NN model has been proposed to solve the same age-old problem, that is, MPP tracking (Tsai et al., 2008) (Messalti et al., 2015). The main challenge in using NN models lies in training them properly, and hence, the novelty of this study lies in tackling that challenge successfully.

This study successfully fulfilled the authors’ ultimate research target of creating a fundamental framework for MPPT with the help of artificial intelligence (AI). The main contributions of this study are:

- 1) The complete dataset was prepared in such a way that it eliminates data bias while supporting a wide range of temperature and irradiance. Extra care has been taken to make it free from overfitting.
- 2) To ensure higher accuracy than the existing models, the supervised machine learning approach is taken for this robust MPPT model.

Some existing models use the data required to generate the ANN network obtained from the principle of the perturbation and observation (P&O) method. Consequently, it pertains to the errors that are generated from the P&O method (Messalti et al., 2015). The error back propagation method is also used in some models to train the neural network. But in our model, we took a basic approach and used the basic equations of a solar cell circuit model which is why the chances of in-built errors are taken care of very well. Also, hardware support has been added to add to the reliability of the simulation results.

The organization of the study is as follows:

- In Section 2, a detailed theoretical analysis of our proposed model is provided since this base information will be used in the experiments, especially in the schematic design.
- In Section 3, the design of the MPPT model has been provided.
- The experimental results are described with rigorous analysis in Section 4.
- Lastly, the study concludes in acknowledgement and referencing recent related research works.

2 Theoretical analysis of the proposed method

2.1 Temperature dependence and effect of irradiance

While using any form of renewable energy, how it impacts nature and how nature has its impact on it are some things we

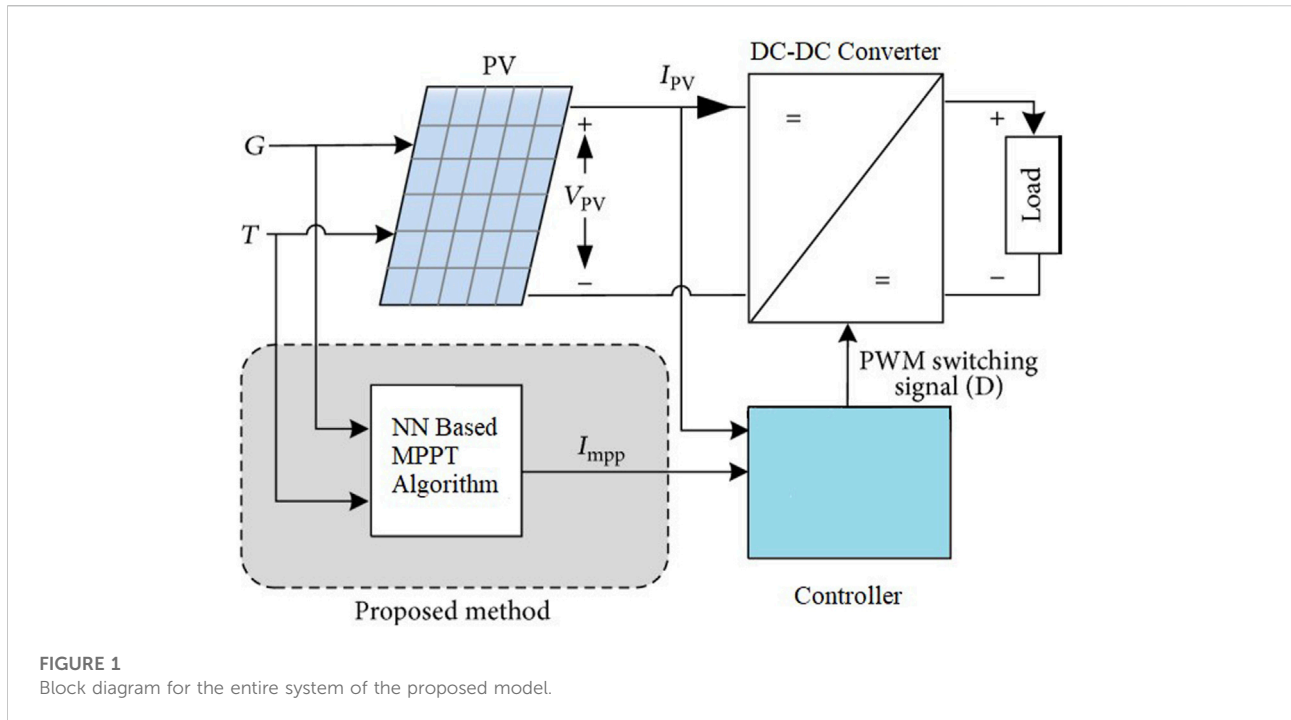


FIGURE 1
Block diagram for the entire system of the proposed model.

must keep under consideration. The same goes for using solar energy as a power source. As the intensity of solar power depends directly on the irradiance and temperature, we must consider the environmental factors while extracting the maximum power from solar panels.

The duration and intensity of sunlight that strikes the surface of the PV panel directly control the numerical value of the output current (Avila et al., 2017) (Subha and Himavathi, 2014). This explains the reason for the popularity of solar energy as a form of renewable energy in countries which are mostly tropical. But unlike the output current, the output voltage does not undergo such direct changes due to the change in irradiance.

The one factor that mostly affects the output voltage and power is temperature. The relation between temperature and output voltage is linear, so to increase the output voltage, a higher temperature is preferable. As extra power in PV modules is decreased in high temperatures, the advantage of MPPT charge controllers also decreases. Hence, even at normal operating temperatures, the additional unused power of an MPPT charge controller compared to a PWM controller can be minimal.

2.2 Schematic of the base maximum power point tracking model

The main focus of this study is on developing the controller rather than designing the DC-DC converter. The problem is in the supervised machine learning domain, and we used regression to predict the value of the maximum power point current (I_{mpp})

to track the maximum power point for a given irradiance G and temperature T (Sedaghati et al., 2012).

Figure 1 shows that G and T are inputs for the PV panel which generates the panel voltage (V_{PV}) and drives the panel current (I_{PV}) to a DC-DC converter and a controller. The MPPT controller compares the value of the maximum power point current (I_{mpp}) with I_{PV} and generates the PWM switching signal (D) for the DC-DC converter to deliver maximum power to the load. Since there are multiple input variables, this will be multivariate regression (Sinha et al., 2014). Coupling to the load to transfer the maximum power requires providing a higher voltage or higher current. Usually, a buck-boost scheme or sometimes a buck converter is used with a voltage and a current sensor tied to a feedback loop using a controller to vary the switching times of the switching signal (Chauhan and Prakash, 2018).

But in conventional MPPT algorithms, boost-type DC-DC converters are used instead of the buck topology since they can switch between two different operating modes—the MPPT mode and the voltage level control mode. Once the maximum available solar power is drawn from the photovoltaic cells by the MPPT controllers, DC-DC converters convert the voltage from one level to another to deliver the maximum power to the load.

2.3 Parameters of the solar module in simulation

Our study uses a simple and basic equivalent circuit model for the solar PV cell comprising a real diode. The diode is placed

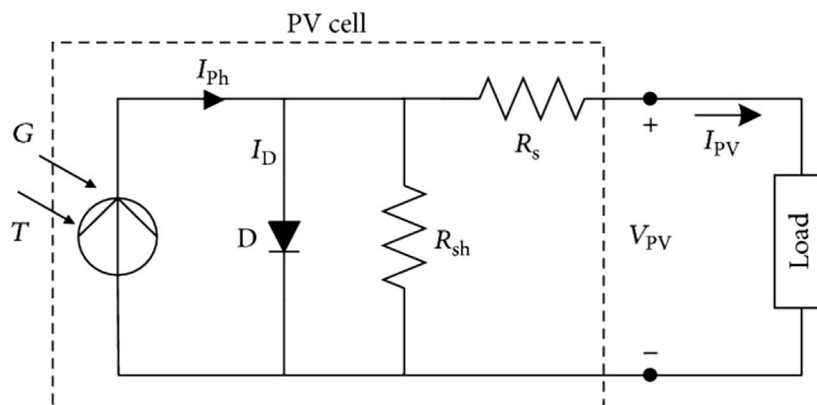


FIGURE 2
Electrical equivalent model of the solar cell.

in parallel with a current source but the current source is an ideal one. The ideal current source supplies current which is in proportion to the irradiance to which it is exposed. There are two conditions of interest for the actual PV and for its equivalent circuit. The first one is the current that flows when the terminals are shorted together (the short-circuit current, I_{sc}). The second one is the voltage across the terminals when the leads are left open (the open-circuit voltage, V_{oc}).

In most real cases, a more robust PV equivalent circuit model is required where some resistive elements accounting for power losses, for example, a parallel leakage (or shunt) resistance R_{sh} and a series resistance R_s are included. Such a circuit is used in this study and is shown in Figure 2. In Figure 2, the electrical equivalent model for the solar cell takes G and T as inputs and produces I_{ph} which flows through three different branches. One portion of the current goes through a branch containing the diode, the other two portions flow through the two types of resistances (Tamrakar et al., 2015). The current produced from the solar PV panel, I_{pv} is then supplied to the load.

Here, I_{ph} is the photocurrent produced by solar power, V_{pv} and I_{pv} are the voltage and the current measured at the output terminal generated from the solar PV panel, respectively, R_{sh} and R_s are shunt and series resistances, respectively, I_D is the diode current, and D is used to denote the diode.

Each solar panel or module is rated to produce a certain portion of wattage, a fixed amount of voltage, and a definite level of amperage under specific conditions (such as irradiance, air mass, and cell temperature). But in ideal cases, all cells possess similar characteristics with no mismatching losses (Peng et al., 2013). The electrical characteristics of the PV module that are used in this study along with temperature are shown in Table 1.

Here, n is used to denote the number of series-connected solar cells in the PV array, R_s and R_{sh} stand for series and shunt resistances, respectively, I_{sc} and V_{oc} are used for short-circuit

TABLE 1 PV module characteristics.

Parameter	Value
N	54
R_s (Ω)	0.2210
R_{sh} (Ω)	415.4050
I_{sc} (A)	8.21
V_{oc} (V)	32.9
T ($^{\circ}C$)	25

current and open-circuit voltage, respectively, and T is used to denote atmospheric temperature.

2.4 Building blocks of the base model

The first step of creating the base model for making the database and mathematical modelling of solar PV array in MATLAB/Simulink requires the use of different equations for obtaining the values of different electrical characteristics of the equivalent circuit model.

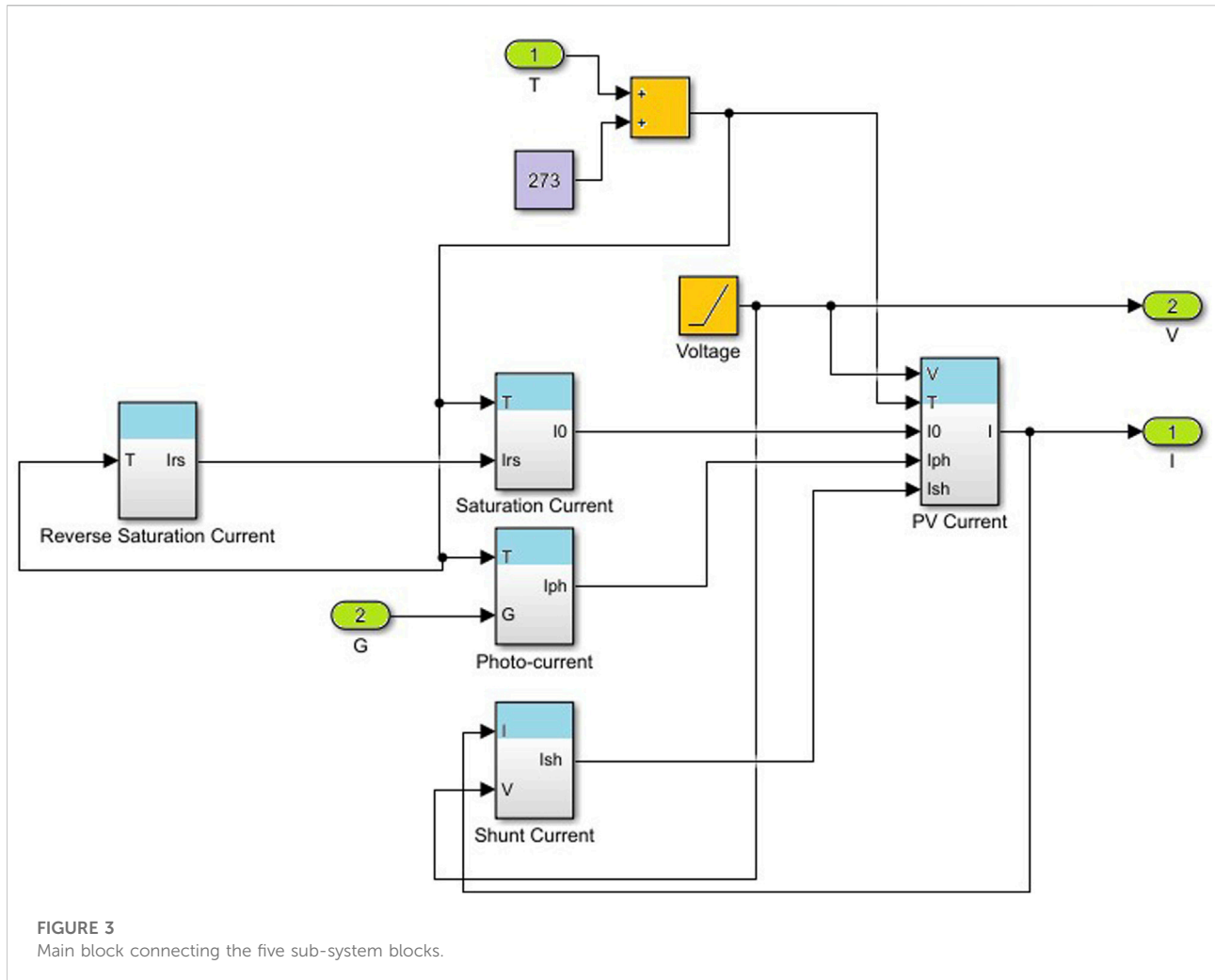
The required equations for the five sub-system blocks of the main Simulink block are given as follows.

Photo current:

$$I_{PH} = \frac{\{I_{SC} + K_I (T - 298)\}G}{1000} \tag{1}$$

Here, I_{PH} : photo-current (A); I_{SC} : short-circuit current (A); K_I : short-circuit current of the cell at $25^{\circ}C$ or 298K and 1000 W/m^2 ; T : operating temperature (K); and G : solar irradiation (W/m^2).

Saturation current:



$$I_0 = \left(\frac{I_{RS} \times T^3}{T_N^3} \right) e^{\left\{ \frac{q E_{G0} \left(\frac{1}{T_N} - \frac{1}{T} \right)}{nk} \right\}} \tag{2}$$

Here, T_N : nominal temperature = 298.15 K; E_{G0} : band gap energy of the semiconductor = 1.1 eV; q : electron charge = 1.6×10^{-19} C; n : ideality factor of the diode; and K : Boltzmann’s constant, = 1.3805×10^{-23} J/K.

Reverse saturation current:

$$I_{RS} = \frac{I_{SC}}{e^{\left(\frac{q \times V_{OC}}{m \times N_s \times k \times T} \right)} - 1} \tag{3}$$

Here, V_{oc} : open-circuit voltage (V) and N_s : number of cells connected in series.

Current through shunt resistance (shunt current):

$$I_{SH} = \frac{V + I \times R_S}{R_{SH}} \tag{4}$$

Output PV current:

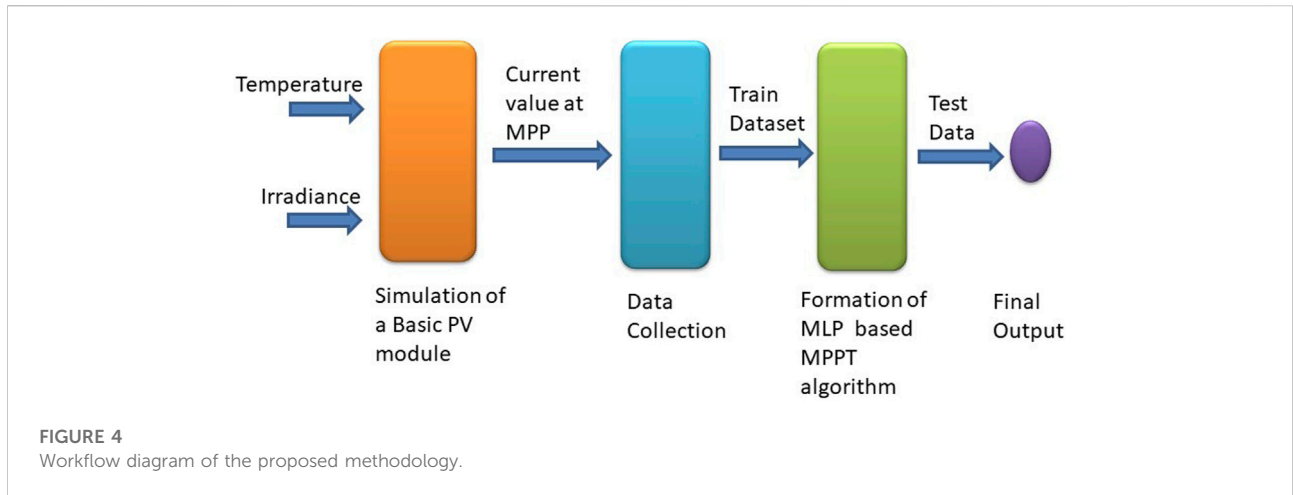
$$I = I_{PH} - I_0 \times I_{SH} \times \left[e^{\left(\frac{q \times (V + I_{RS})}{m \times k \times N_s \times T} \right)} - 1 \right]. \tag{5}$$

The next step is to concatenate the five sub-system blocks and build the main block to obtain the output current and voltage from a solar module. Figure 3 shows that there are, in total, five separate sub-system blocks for reverse saturation current (input T and output I_{RS} or I_{rs}), saturation current (inputs T and I_{RS} , and output I_0), photocurrent (inputs T and G, and output I_{PH} or I_{ph}), shunt current (inputs I, V, and I_{SH} or I_{sh}), and PV current (inputs V, T, I_0 , I_{PH} , and I_{SH} , and output I).

3 Design of the MPPT module

3.1 Proposed methodology

The design of the MPPT module can be divided into three steps as shown in Figure 4. In the first step, the basic PV module



takes temperature and irradiance values as input data and gives the current value at the MPP as output data (Pindi et al., 2020) (Kumar et al., 2019). The second step is data collection which relies on the simulation results from the first step. After the training dataset is created, it can be used to train the proposed multilayer perceptron (MLP)-type artificial neural network (ANN) and obtain the final output from our test data (Jyothy and Sindhu, 2018).

3.2 Simulation results of the base model

The PV array block of the MATLAB Simscape library implements an array of PV modules. The array is built of strings of modules which are connected in parallel, each string comprising modules connected in series. This block allows us to model preset PV modules from the National Renewable Energy Laboratory (NREL) System Advisor Model (Jan. 2014) and the PV modules that we define.

The PV array block is a five-parameter model using a current source I_L (light-generated current), diode (I_0 and n_1 parameters), series resistance R_s , and shunt resistance R_{sh} to represent the irradiance- and temperature-dependent I-V characteristics of the modules. Figure 5 shows that the solar PV module takes T and G as inputs, and then the module generates output current and voltage as denoted by I and V, respectively. The values of I and V are used to generate an I-V graph and P-V graph for better speculation of the MPP of the system.

Now, after simulating the prescribed model, the graphs (I vs. V and P vs. V) derived from this simulation perfectly match the known shapes of PV model outputs.

This implies that this model works correctly and the data obtained from this model can be safely used for further investigation and for training a neural network architecture later on.

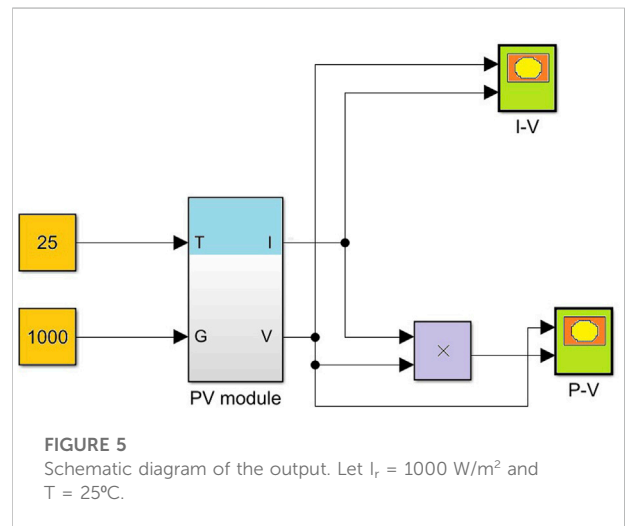
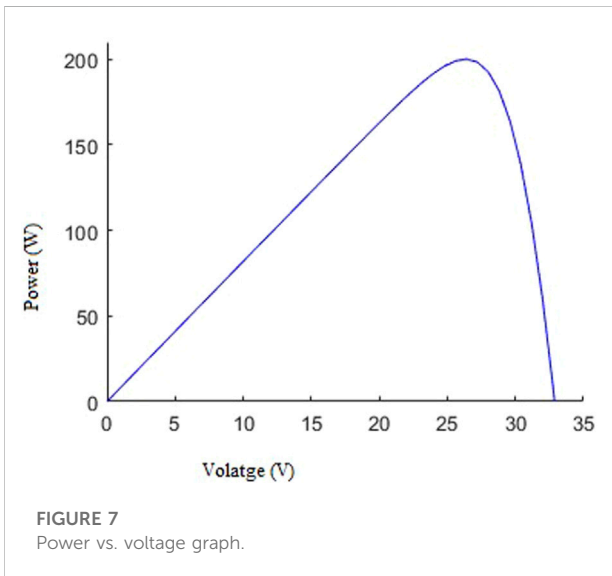
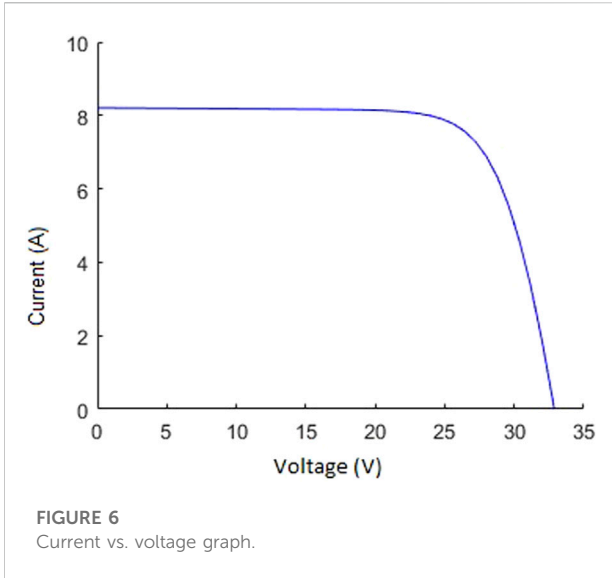


Figure 6 shows the current versus voltage graph which clearly denotes that the MPP, the current value, and the voltage value at the MPP can easily be perceived from this graph.

Figure 7 shows the power versus voltage graph which clearly denotes the MPP, the voltage value corresponding to the highest value of power, denotes V_{mpp} .

We know that any solar cell has I_{sc} (here, 8.1A) and V_{oc} (here, 32.9V) fixed. Here, the values of V_{mp} at P_{max} can manually be found for inputs $T = 25 \text{ K}$ and $G = 1000 \text{ W/m}^2$.

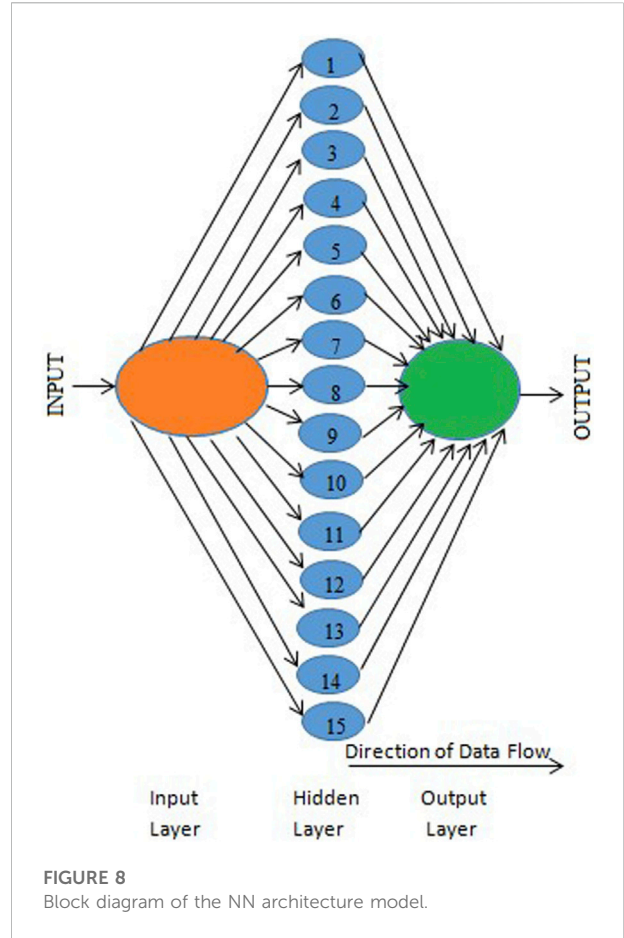
At power $P_{max} = 200.0170 \text{ W}$ (found by scrolling down all the power values, as these are the biggest data among all) at time index = 2.6400, we get $V_{mp} = 26.4000 \text{ V}$ at the corresponding time. This way, the values of T and G can be changed and the corresponding values of V_{mp} at P_{max} are calculated. Finally, the value of the current at the maximum power point (I_{mp}) is obtained from these data or a short MATLAB code can be generated to do the task in a short span of time.



For this cell, every necessary data can be found from the workspace of MATLAB. At this stage, the value of V_{mp} (voltage at maximum power) at P_{max} is required. To collect these data, a simple workaround (Simulation Data Inspector>Log selected Signals) is performed.

3.3 Creation of a customized dataset

After running a total of 1,300 simulations, we created our own dataset for T starting from 15 to 40 units ($40 - 15 + 1 = 26$ values of T); (for each T, the values of G are 200, 210,



220...1,090 etc., totaling in 50 values). In real atmospheric conditions, the difference between the maximum and minimum temperature can be large for a certain geographical area which is taken care of by the large range of temperature values used in the dataset.

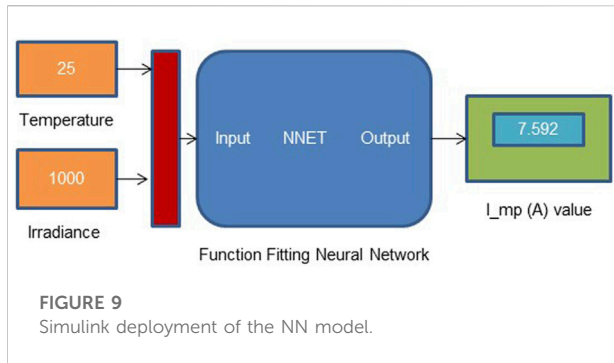
To make the data randomized, they are modified using simple mathematical techniques. This helps prevent data bias for the neural network model. The basic three operations used are shuffling, splitting, and transposing.

Shuffle: all the collected data are shuffled randomly.

Splitting: in this study, the data matrix size is $1,300 \times 3$. Now, the data file is split into two different files:

- 1) The input file includes T and G data;
- 2) the output file includes I_{mp} data.

Transpose: as per the requirement of MATLAB's neural fitting (nftool), the features (i.e., inputs) have to be in the columns of the data matrix. The input matrix must be transposed which includes T and G values. Similarly, the target matrix (i.e., output) must also be transposed. Finally, a



column matrix which includes I_{mp} values can be obtained in this process.

3.4 Fitting data into neural network architecture

In this study, a multilayer feed-forward network was used as the neural network architecture. Here, each layer of nodes receives input data from the previous layers. The outputs of the nodes in one layer are inputs to the next layer. Moreover, the inputs to each node are combined using a weighted linear combination. Finally, the result is modified by a nonlinear function before being output.

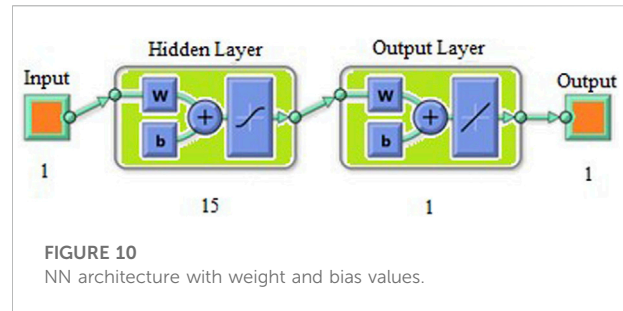
As per definition, this neural network is formed in three layers, called the input layer (passive nodes), hidden layer (active nodes), and output layer (active nodes); the first layer is the input and the last layer is the output. Figure 8 shows that the neural network architecture used in this model comprises 15 hidden neurons in the hidden layer.

In this MLP NN, adaptive moment estimation (Adam) has been used as the optimization algorithm instead of the classical stochastic gradient descent procedure (Salah and Fourati, 2019). For the loss function, the mean squared error (MSE) method has been applied. The number of epochs and the value of the learning rate are 1,000 and 0.001 s (approximately), respectively.

At first, both the input (two variables) and output (two variables) data files were loaded. Then, 5% of our data was selected as the test dataset which includes 65 samples, 85% data as the training dataset which includes 1,105 samples, and 10% data as the validation dataset which includes 130 samples.

3.5 Use of Bayesian-regularized artificial neural networks for regression analysis

Bayesian neural networks (BNNs) are important in specific settings, particularly when the factor of uncertainty is taken care of. Some examples of these cases are decision-making



systems, (relatively) smaller data settings, Bayesian optimization, model-based reinforcement learning, and other similar areas.

In our model of MPPT, we used Bayesian regularized artificial neural networks (BRANNs) because of their higher level of robustness compared with standard back-propagation nets. Another reason for using the BRANN is that it can lessen or eliminate completely the need for lengthy cross-validation. In fact, Bayesian regularization is a very sturdy mathematical tool that converts a nonlinear regression into a well-posed statistical problem statement in the manner of ridge regression. Hence, the Bayesian regularization method was chosen as the training algorithm as it works best even for smaller data.

4 Experimental results

After creating and training the network, a very small mean square value of error was observed which ensures the effectiveness of the model. The MSE value for testing is very low ($\sim 2.87 \times 10^{-3}$) for the proposed model.

4.1 Simulink deployment

Simulink deployment of the model has made it a very handy tool which instantly shows the MPP after setting the input parameters. Moreover, the time lag to generate the output is very negligible, hence establishing the model as a fast one.

Figure 9 shows that if we insert T and G values (here, $T = 25^\circ$ and $I_r = 1000 \text{ W/m}^2$) as inputs to the function fitting the NN model, it instantly shows the corresponding current value at the MPP (here, $I_{mp}(A)$ value = 7.592 A).

4.2 Bias values and weight values in the neural network architecture

As an additional parameter, bias values in the NN architecture help adjust the output along with the weighted sum of the inputs to the neuron. Another important use of

TABLE 2 Bias values of input in the hidden layer.

Bias values for input in the hidden layer

-0.0788662358905827
-0.199252461268044
0.476703785811994
0.0788437136945187
0.0788437137489292
-0.0843897428619086
0.0788437137616096
-0.0788437136323596
0.0788437137854139
-0.0511645156192877
0.0521386721602554
0.0788437137594562
0.0788437137550028
0.325165283314198
0.199252475098178

bias values is that they help shift the activation function in either the right or left direction. Bias values for the input in the hidden layer are portrayed in the following table. Figure 10 shows the NN architecture which takes the input for the inner hidden layer, then comes the output layer, and finally, the output can be obtained at the last stage. W and B indicate the weight values and the bias values, respectively.

All the bias values and weight values can be readily obtained from the model and are mentioned in Tables 2–4 which will make the hardware implementation of the proposed MPPT model possible in no time.

Another important parameter in the NN architecture is the weights, which represent the strength of the connection between units. If the weight value of node 3 is higher than that of node 4, neuron 3 has a higher influence over neuron 4. Hence, weight values can bring down the importance of the input values. Weights of input in the hidden layer are given in the following table.

In an NN model, a neuron first computes the weighted sum of the inputs. For the inputs $(x_1, x_2, x_3, \dots, x_n)$ and the weights $(w_1, w_2, w_3, \dots, w_n)$, a weighted sum is computed as

$$x_1w_1 + x_2w_2 + x_3w_3 \dots + x_nw_n.$$

Subsequently, a bias (constant) is added to the weighted sum.

$$x_1w_1 + x_2w_2 + x_3w_3 \dots + x_nw_n + \text{Bias}.$$

Finally, the computed value is fed into the activation function, which then prepares an output.

$$\text{Output, } Y = \Sigma (\text{Weight} \times \text{Input}) + \text{Bias}.$$

$$\text{Activation function: } (x_1w_1 + x_2w_2 + x_3w_3 \dots + x_nw_n + \text{Bias})$$

These functions are mathematical tools that can normalize the inputs.

TABLE 3 Weights of input in the hidden layer.

T	G
0.330659943126136	0.375354867765757
-0.243061055602675	-0.302898742825237
-0.413686729890811	0.124969405112560
0.0503908825102565	-0.242889973645394
0.0503908825336595	-0.242889973660344
0.286942170255656	-0.871006037765083
0.0503908825390176	-0.242889973663920
-0.0503908824834618	0.242889973628136
0.0503908825490957	-0.242889973670382
-0.194105547886448	-0.882406133751217
-0.685142210229390	0.629560967118233
0.0503908825379756	-0.242889973663218
0.0503908825362639	-0.242889973662112
0.796782784260382	-0.181097405343480
0.243060836205972	0.302898505989682

4.3 Checking the accuracy of the result

Bin represents the number of vertical bars observed on the graph. Figure 11 shows that the total error from the neural network ranges from 0.2222 (leftmost bin) to 0.1968 (rightmost bin). This error range is divided into 20 smaller bins, so each bin has a width of $[0.1968 - (-0.2222)]/20 = 0.02095$.

Each vertical bar represents the number of samples from the dataset, which lies in a particular bin. For example, on the left half of the graph, there is a bin corresponding to the error of -0.07468 and the height of that bin for the validation dataset is 200.

It means that 200 samples from the dataset (training + test) have an error which lies in the following range:

$$[(-0.07468 - 0.02095/2), (-0.07468 + 0.02095/2)]$$

The range (-0.012135, 0.008815) is even less than the range of the bin corresponding to -0.07468.

Figure 12 shows three plots for the regression analysis, the plot for the training data shows that only one data point deviates from the line of regression, the plot for the test data shows that almost all the data points are either on or very close to the line of regression, and there is an overall third plot for the whole dataset.

The result of the regression analysis is as follows:

- 1) Training: only one data point deviated from the locus of the straight line.
- 2) Test: no data point deviated from the locus of the straight line.
- 3) Validation: error was zero for the validation dataset.

4.3.1 Verification

Although this model is a software-based one, it was implemented in a hardware setting to check the acceptability

TABLE 4 Weights in the output layer.

Weights in the output layer

0.526055556926590
-0.526712907336645
0.560221719680131
-0.357268781908311
-0.357268781972241
-0.335049187325717
-0.357268781987367
0.357268781834757
-0.357268782015078
0.371791504344763
-0.318328545469931
-0.357268781984634
-0.357268781979911
-0.244907095063019
0.526712952341475

TABLE 5 Solar panel specifications.

Parameter	Value
Model type	ZM-A-M-100
Cell type	156 mm × 104 mm
Cell arrangement	36 cells in series
Dimensions (mm)	1,006 mm × 676 × 30 mm
Material	Monocrystalline silicon
Maximum power	100 W
Number of cells	36 pcs

of the results (Mujumdar and Tutkane, 2013) (Hwang et al., 2019). Figure 13 shows the simple hardware set-up where one solar panel, one lead-acid battery (100AH), two rheostats, two multimeters, cables, and one solar panel controller were used. Also, a boost regulator was used here, and the bias values and the weight values were used with the help of an Arduino board. The dimensions of the panel were 1006 × 676 × 30 mm, and the other panel specifications are as follows. Table 5 states the solar panel specifications used in the hardware experiment.

4.3.2 Analysis

Since the proposed NN model is a simple one-layer network, it can be implemented in real-time. Also, temperature and irradiance values do not change rapidly in real environmental conditions (Rezk et al., 2020). Hence, the timing analysis shows that it takes only around 1 millisecond to produce the output, thus proving the model to be very time efficient.

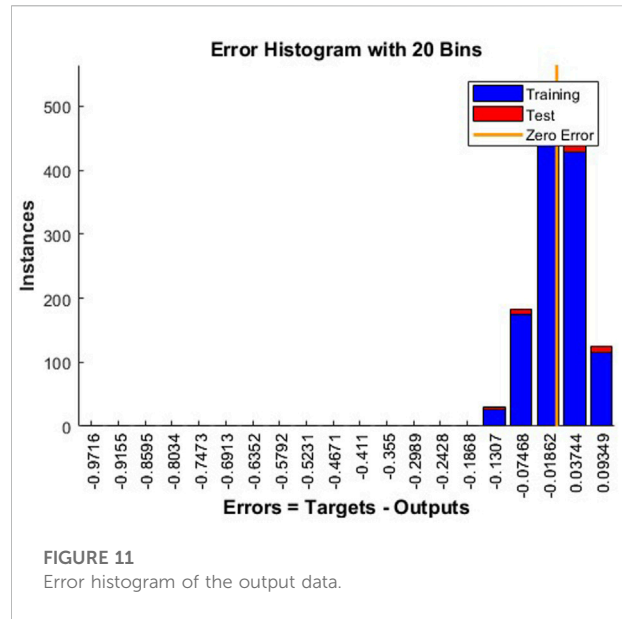


FIGURE 11 Error histogram of the output data.

In real-time settings, noise gets added in every step of the MPPT analysis procedure, for example, while receiving input data through the sensors. Moreover, human errors also get involved during manual data collection. To counter this noise issue, some additive white Gaussian noise (AWGN) was added during the training phase, and then finally trained the model with the data corresponding to the clean result and received better performance with test data. So, it shows less discrepancy even with very noisy data, thus adding to the robustness of the model.

For countries with extreme weather conditions, the difference between the maximum temperature value in the summer and the minimum temperature value in the winter can be a large number. In such cases, the dataset used in this study can easily be modified and some temperature values close to the maximum and minimum temperature values of that specific region of the world can be added. Similar tasks can be done for varying irradiance levels in remote places of the world. This is easy but important modifications of the dataset can add to the flexibility of the model.

The simplest method for MPPT analysis so far has been the P&O method but the proposed model, being a very simple feed-forward network, can easily replace the P&O method.

The low-cost hardware set-up proves that this model is very cost-effective.

4.3.3 Performance comparison

Discrepancy: from the simulation data, for T = 25 K and G = 1000 W/m², Imp = 7.5764 A but the neural network model produces Imp = 7.592 A. The percentage of deviation from simulation data= (7.592-7.5764)/7.5764 × 100% = 0.206%.

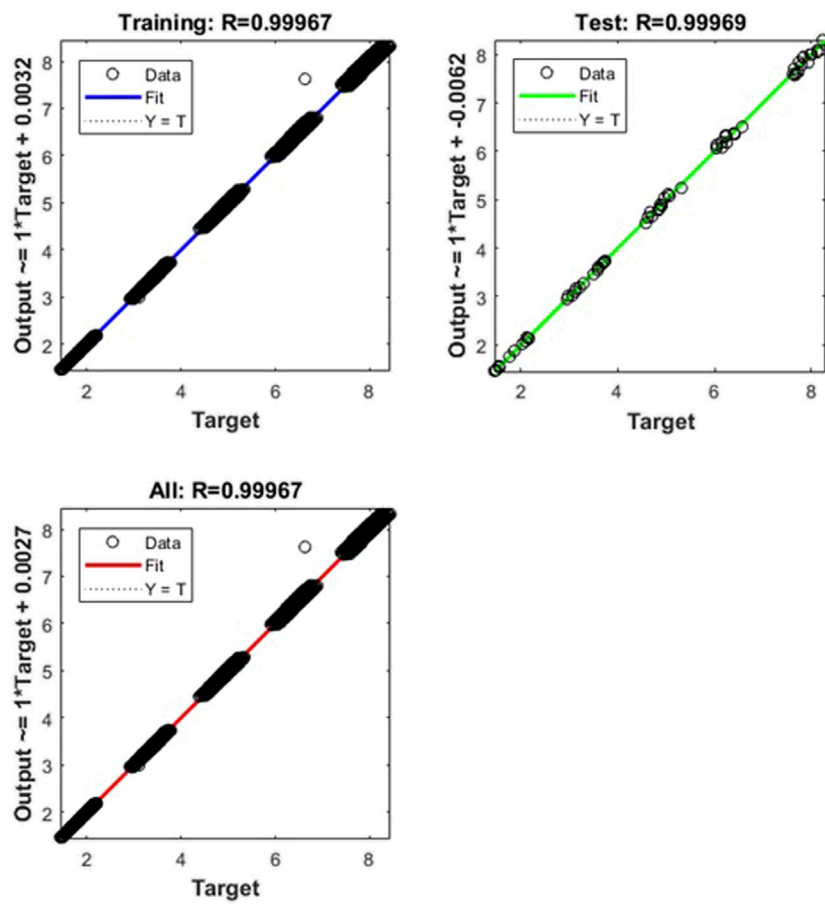


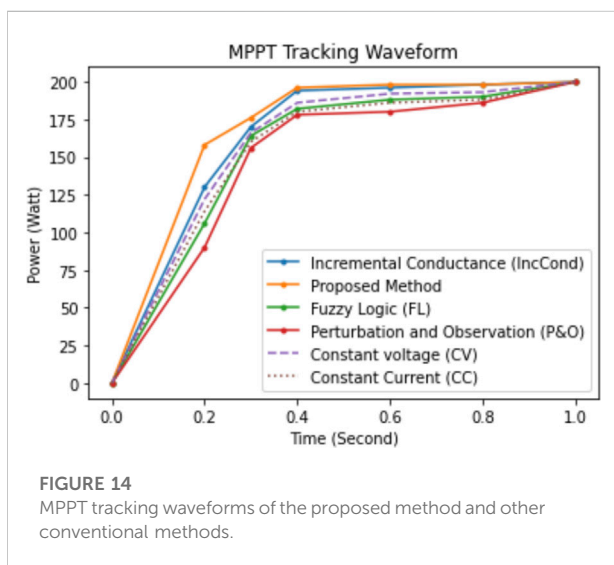
FIGURE 12
Plot for regression analysis.



FIGURE 13
Full hardware set-up.

TABLE 6 Comparison with other conventional and popular MPPT methods.

MPPT method	Type	Complexity level	Convergence speed	Prior training	Efficiency (%)	Sensed parameter	Cost	Automation
P and O	Online	Low	Low	No	67.4	V and I	Easily affordable	No
Inc Cond	Online	Medium	Varies	No	81.39	V and I	Less expensive	No
CV	Online	Medium	Varies	No	75.35	V	Less expensive	No
CC	Online	Medium	Varies	No	80.61	I	Less expensive	No
FL	AI	High	Fast	Yes	90.08	V and I	Expensive	Yes
Proposed method	AI	Low	Fast	Yes	99.80	V and I	Easily affordable	Yes



So, this neural network model for tracking the maximum power point is very effective. Increasing the number of neurons in the hidden layer gives even better results (by adjusting network size). This model data was used to calculate the accuracy also.

4.3.4 Efficiency

Percentage of accuracy of the model data = $(1 - 0.206\%) = 99.794\%$. This high accuracy is one of the novelties of this study. The size of the hidden layers to produce such a close approximation of the MPP is only 15.

For this same environmental condition, other popular and easy-to-implement methods give much lesser efficiency, for example, P&O has an accuracy level of 67.4%. The efficiency slightly increases in the case of the IC method (above 80%) but nowhere near compared to our NN model. If the fuzzy logic-based algorithm is used, the efficiency can be increased up to as high as 96% despite the model becoming very complex to implement and the time-lag becoming a major concern (Chim et al., 2011; Baraskar et al., 2016; Narendiran et al., 2016).

Usually, the NN models show an efficiency of around 98%. But the proposed model shows a higher efficiency (99.8% approximately) than even the other existing NN models of MPPT analysis for the same temperature and irradiance value. So, the improvement is approximately ~ 2% for just one solar panel (comprising 36 pieces of cells).

This information is obvious from Table 6, which represents the comparison between the proposed method in this study and other popular and conventional MPPT methods, namely perturb and observe (P&O), incremental conductance (IncCond) method, constant voltage (CV), constant Current (CC), and fuzzy logic (FL). Being an ML-based method, along with the advantage of automation, the proposed model is cost-effective and time-efficient. Fuzzy logic-based algorithms are automated and have fast convergence speed, but they are usually computationally costly. For a better comparison among the methods, MPPT tracking waveforms are shown in Figure 14.

Clearly, our proposed method performs more efficiently than the other traditional approaches. For different partial shading settings, these MPPT tracking waveforms follow a similar pattern. However, we did not include any hybrid algorithm to keep our proposed model computationally inexpensive, easy to implement, and cost-effective.

5 Conclusion and scope of the future work

In this study, an overall schematic diagram of a photovoltaic system is designed. By analyzing the output characteristic of a solar cell, an improved MPPT algorithm on the basis of the NN method is put forward to track the MPP of solar cell modules. The theoretical results show that the improved NN MPPT algorithm has higher efficiency than the P&O method in the same environment, and the photovoltaic system can keep working at the MPP without oscillation and misjudgment. So, it can not only reduce misjudgment but also avoid power loss around the MPP.

There are two major limitations of this proposed method. First, the work in this study does not consider variable load conditions. However, load variation will be included as another input parameter to the proposed NN model in the future work of these authors (Shams et al., 2021a) (Shams et al., 2021b; Chtita et al., 2022). Second, in the hardware setup, there is no motion control for partial shading (Fares et al., 2021) (Pervez et al., 2021). A decent future research idea might be to adjust the hardware setup to incorporate a smart system to work efficiently in different partial shading conditions.

The experiments were done in the capital city of a tropical, fast-developing country (Dhaka, Bangladesh), where using solar power is quite significant considering the poor economic condition of many people (Thentral et al., 2022) (Mirza et al., 2022). Therefore, the cost-effectiveness of a realistic MPPT approach is vital for real-life implementation and our method can track the maximum power point without adding to any significant installment cost. Also, the same experiments have been repeated in other major cities (Rajshahi, Sylhet, and Chittagong) of Bangladesh to include environmental variability, and similar results have been reported.

Since this is a “Supervised Machine Learning”-based approach, the training and testing dataset has been made publicly available on the “HARVARD DATAVERSE” website. This is to ensure the reproducibility of the results presented in this work. Dataset link: <https://doi.org/10.7910/DVN/IH6AC2>. In case of any technical problems on the website, the dataset might be provided upon request by the corresponding author. Moreover, how this dataset has been created and how it is used to train and test our ML model has been described in great detail in Section 3. Therefore, this scheme makes it a reproducible work. Different irradiance levels and partial shading conditions have been incorporated into the new dataset (will be published soon) so that this same model can be trained and tested using the revised dataset without altering any experimental setting mentioned in this study. Supervised machine learning (ML) is used in solar systems when the target feature (output) is known or available (Alloghani et al., 2020). In the case of our proposed method,

- 1) The ground truth dataset has been created using a conventional and popular MPPT approach. Since it is a customized dataset, it performs very efficiently for a particular geographical region and similar customized datasets can be created using the same steps for other geographical areas, which makes this procedure overall generalized in nature.
- 2) This dataset has been used to train our proposed supervised ML model and the test accuracy proves that this model can predict the MPP very efficiently. This method is computationally inexpensive and easily applicable in real-life settings. Otherwise, in the absence of the target feature

variable, unsupervised ML models will be appropriate for training, validating, and testing.

Data availability statement

The datasets presented in this study can be found in online repositories. The names of the repository/repositories and accession number(s) can be found at: <https://dataverse.harvard.edu/dataset.xhtml?persistentId=doi:10.7910/DVN/IH6AC2>.

Author contributions

All authors listed have made a substantial, direct, and intellectual contribution to the work and approved it for publication.

Funding

This project was not funded, and the authors have no conflict of interest. This research work is dedicated to KR, who was a renowned Professor of Bangladesh University of Engineering and Technology (BUET) and died at the onset of pandemic after suffering from COVID-19.

Conflict of interest

The authors declare that the research was conducted in the absence of any commercial or financial relationships that could be construed as a potential conflict of interest.

Publisher's note

All claims expressed in this article are solely those of the authors and do not necessarily represent those of their affiliated organizations, or those of the publisher, the editors, and the reviewers. Any product that may be evaluated in this article, or claim that may be made by its manufacturer, is not guaranteed or endorsed by the publisher.

Supplementary material

The Supplementary Material for this article can be found online at: <https://www.frontiersin.org/articles/10.3389/fenrg.2022.932653/full#supplementary-material>

References

- Alloghani, M., Al-Jumeily, D., Mustafina, J., Hussain, A., and Aljaaf, A. J. (2020). "A systematic review on supervised and unsupervised machine learning algorithms for data science," in *Supervised and unsupervised learning for data science. Unsupervised and semi-supervised learning*. Editors M. Berry, A. Mohamed, and B. Yap. (Cham: Springer). doi:10.1007/978-3-030-22475-2_1
- Avila, E., Pozo, N., Pozo, M., Salazar, G., and Dominguez, X. (2017). "Improved particle swarm optimization based MPPT for PV systems under Partial Shading Conditions," in *IEEE Southern Power Electronics Conference (SPEC)*, 04-07 December 2017 (Puerto Varas, Chile: IEEE). doi:10.1109/spec.2017.8333634
- Azad, M. L., Das, S., Kumar Sadhu, P., Satpati, B., Gupta, A., and Arvind, P. (2017). "P&O algorithm based MPPT technique for solar PV system under different weather conditions," in *International Conference on Circuit, Power and Computing Technologies (ICCPCT)*, 20-21 April 2017 (Kollam, India: IEEE).
- Baraskar, S., Jain, S. K., and Padhy, P. K. (2016). "Fuzzy logic assisted P&O based improved MPPT for photovoltaic systems," in *2016 International Conference on Emerging Trends in Electrical Electronics & Sustainable Energy Systems (ICETEES)*, 11-12 March 2016 (Sultanpur, India: IEEE), 250–255. doi:10.1109/ICETEES.2016.7581369
- Barua, N., Dutta, A., Chakma, S., Das, A., and Chowdhury, S. S. (2016). "Implementation of cost-effective MPPT solar photovoltaic system based on the comparison between Incremental Conductance and P&O algorithm," in *IEEE International WIE Conference on Electrical and Computer Engineering (WIECON-ECE)*, 19-21 December 2016 (Pune, India: IEEE), 143–146.
- Chekired, F., Larbes, C., Rekioua, D., and Haddad, F. (2011). Implementation of a MPPT fuzzy controller for photovoltaic systems on FPGA circuit. *Energy Procedia* 6, 541–549. doi:10.1016/j.egypro.2011.05.062
- Chauhan, A. S., and Prakash, S. (2018). "Considering various equivalent circuits for solar PV array modelling," in *2018 2nd International Conference on Power, Energy and Environment: Towards Smart Technology (ICEPE)*, 01-02 June 2018 (Shillong, India: IEEE), 1–6. doi:10.1109/EPETSG.2018.8658741
- Chim, C. S., Neelakantan, P., Teo, H. P. K. T. K., and Teo, K. T. K. (2011). "Fuzzy logic based MPPT for photovoltaic modules influenced by solar irradiation and cell temperature," in *2011 UKSim 13th International Conference on Computer Modelling and Simulation*, 30 March 2011 - 01 April 2011 (Cambridge, UK: IEEE), 376–381. doi:10.1109/UKSIM.2011.78
- Chitta, S., Motahhir, S., El Hammoumi, A. E., Chouder, A., Benyoucef, A. S., El Ghzizal, A. E., et al. (2022). A novel hybrid GWO-PSO-based maximum power point tracking for photovoltaic systems operating under partial shading conditions. *Sci. Rep.* 12 (1), 10637. doi:10.1038/s41598-022-14733-6
- de Brito, M. A. G., Galotto, L., Sampaio, J. L. P., e Melo, G. A., and Canesin, C. A. (2013). Evaluation of the main MPPT techniques for photovoltaic applications. *IEEE Trans. Ind. Electron.* 60 (3), 1156–1167. doi:10.1109/tie.2012.2198036
- Esrasm, T., and Chapman, P. L. (2007). Comparison of photovoltaic array maximum power point tracking techniques. *IEEE Trans. Energy Convers.* 22 (2), 439–449. doi:10.1109/tec.2006.874230
- Fares, D., Fathi, M., Shams, I., and Mekhilef, S. (2021). A novel global MPPT technique based on squirrel search algorithm for PV module under partial shading conditions. *Energy Convers. Manag.* 230, 113773. doi:10.1016/j.enconman.2020.113773
- Frezza, A., Manfredi, S., and Suardi, A. (2014). Adaptive FOCV-based control scheme to improve the MPP tracking performance: An experimental validation. *IFAC Proc. Vol.* 47 (3), 4967–4971. doi:10.3182/20140824-6-za-1003.02464
- Hohm, D. P., and Ropp, M. E. (2002). "Comparative study of maximum power point tracking algorithms," in *Conference Record of the Twenty-Eighth IEEE Photovoltaic Specialists Conference - 2000 (Cat. No.00CH37036)*, 15-22 September 2000 (Anchorage, AK, USA: IEEE). doi:10.1002/pip.459
- Hwang, K., Lee, K., and Kim, I. (2019). "A high speed solar MPPT controller design," in *2019 IEEE 28th International Symposium on Industrial Electronics (ISIE)*, 12-14 June 2019 (Vancouver, BC, Canada: IEEE), 1029–1034. doi:10.1109/ISIE.2019.8781420
- Ibrahim, O., Yahaya, N. Z., Saad, N., and Umar, M. W. (2015). "Matlab/Simulink model of solar PV array with perturb and observe MPPT for maximising PV array efficiency," in *IEEE Conference on Energy Conversion (CENCON)*, 19-20 October 2015 (Johor Bahru, Malaysia: IEEE). doi:10.1109/cencon.2015.7409549
- Jyothy, L. P., and Sindhu, M. R. (2018). "An artificial neural network based MPPT algorithm for solar PV system," in *2018 4th International Conference on Electrical Energy Systems (ICEES)*, 07-09 February 2018 (Chennai, India: IEEE), 375–380. doi:10.1109/ICEES.2018.8443277
- Kumar, A., Saha, P. K., and Rao, S. D. V. S. K. (2019). "Cascaded artificial neural network based MPPT algorithm for PV application," in *2019 3rd International conference on Electronics, Communication and Aerospace Technology (ICECA)*, 12-14 June 2019 (Coimbatore, India: IEEE), 296–300. doi:10.1109/ICECA.2019.8821949
- Li, J., and Wang, H. (2009). "Maximum power point tracking of photovoltaic generation based on the fuzzy control method," in *International Conference on Sustainable Power Generation and Supply*, 06-07 April 2009 (Nanjing, China: IEEE).
- Mayatake, M., Veerachary, M., and Toriumi, F. (2011). "Maximum power point tracking of multiple photovoltaic arrays: A particle swarm optimization approach," in *IEEE Transactions on Aerospace and Electronic Systems (IEEE)*, 367–380. doi:10.1109/TAES.2011.5705681
- Messalti, S., Harrag, A. G., and Loukriz, A. E. (2015). "A new neural networks MPPT controller for PV systems," in *Renewable Energy Congress (IREC) 2015 6th International*, 24-26 March 2015 (Sousse, Tunisia: IEEE), 1–6. doi:10.1109/irec.2015.7110907
- Mirza, A. F., Haider, S. K., Ahmed, A., Rehman, A. U., Shafiq, M., Bajaj, M., et al. (2022). Generalized regression neural network and fitness dependent optimization: Application to energy harvesting of centralized TEG systems. *Energy Rep.* 8, 6332–6346. doi:10.1016/J.EGYR.2022.05.003
- Motahhir, S., El Hammoumi, A., and El Ghzizal, A. E. (2020). The most used MPPT algorithms: Review and the suitable low-cost embedded board for each algorithm. *J. Clean. Prod.* 246, 118983. doi:10.1016/j.jclepro.2019.118983
- Mujumdar, U. B., and Tutkane, D. R. (2013). "Development of integrated hardware set up for solar photovoltaic system monitoring," in *2013 Annual IEEE India Conference (INDICON)*, 13-15 December 2013 (Mumbai, India: IEEE), 1–6. doi:10.1109/INDICON.2013.6725944
- Narendiran, S., Sahoo, S. K., Sahoo, R. A. K., and Sahoo, A. K. (2016). "Fuzzy logic controller based maximum power point tracking for PV system," in *2016 3rd International Conference on Electrical Energy Systems (ICEES)*, 17-19 March 2016 (Chennai, India: IEEE), 29–34. doi:10.1109/ICEES.2016.7510590
- Peng, W., Zeng, Y., Gong, H., Leng, Y., Hu, Y. W., Hu, W., et al. (2013). Evolutionary algorithm and parameters extraction for dye-sensitised solar cells one-diode equivalent circuit model. *Micro & Nano Lett.* 8 (2), 86–89. doi:10.1049/mnl.2012.0806
- Pervez, I., Shams, I., Mekhilef, S., Sarwar, A., Tariq, M., Alamri, B., et al. (2021). Most valuable player algorithm based maximum power point tracking for a partially shaded PV generation system. *IEEE Trans. Sustain. Energy* 12 (4), 1876–1890. doi:10.1109/tste.2021.3069262
- Pindi, N., Joshi, S., and Mehta, B. (2020). "Neural Network based MPPT system for Standalone PV system," in *IECON 2020 The 46th Annual Conference of the IEEE Industrial Electronics Society*, 18-21 October 2020 (Singapore, Singapore: IEEE), 1866–1871. doi:10.1109/IECON43393.2020.9255164
- Ramirez-Del-Barrio, P. (2017). "Sustainable development through the use of solar energy for productive processes: The Ayllu Solar Project," in *IEEE Global Humanitarian Technology Conference (GHTC)*, 19-22 October 2017 (San Jose, CA, USA: IEEE). doi:10.1109/ghtc.2017.8239310
- Rezk, H., and Eltamaly, A. M. (2015). A comprehensive comparison of different MPPT techniques for photovoltaic systems. *Sol. Energy* 112, 1–11. doi:10.1016/j.solener.2014.11.010
- Rezk, H., Tolba, A. M. A., and Tolba, M. A. (2020). "Performance analysis of solar PV system under shading condition," in *2020 International Youth Conference on Radio Electronics, Electrical and Power Engineering (REEPE)*, 12-14 March 2020 (Moscow, Russia: IEEE), 1–5. doi:10.1109/REEPE49198.2020.9059172
- Salah, L. B. F., and Fourati, F. (2019). "Deep MLP neural network control of bioreactor," in *2019 10th International Renewable Energy Congress (IREC)*, 26-28 March 2019 (Sousse, Tunisia: IEEE), 1–5. doi:10.1109/IREC.2019.8754572
- Sedaghati, F., Nahavandi, A., Badamchizadeh, M. A., Ghaemi, S., and Abedinpour Fallah, M. A. (2012). PV maximum power-point tracking by using artificial neural network. *Math. Problems Eng.* 2012, 1–10. doi:10.1155/2012/506709
- Shams, I., Mekhilef, S., and Tey, K. S. (2021). Improved-team-game-optimization-algorithm-based solar MPPT with fast convergence speed and fast

response to load variations. *IEEE Trans. Ind. Electron.* 68 (8), 7093–7103. doi:10.1109/tie.2020.3001798

Shams, I., Mekhilef, S., and Tey, K. S. (2021). Maximum power point tracking using modified butterfly optimization algorithm for partial shading, uniform shading, and fast varying load conditions. *IEEE Trans. Power Electron.* 36 (5), 5569–5581. doi:10.1109/tpel.2020.3029607

Sinha, D., Das, A. B., Sadhu, D. K. P. K., and Sadhu, P. K. (2014). "Equivalent circuit configuration for solar PV cell," in 2014 1st International Conference on Non Conventional Energy (ICONCE 2014), 16–17 January 2014 (Kalyani, India: IEEE), 58–60. doi:10.1109/ICONCE.2014.6808682

Subha, R., and Himavathi, S. (2014). "Neural network based maximum power point tracking scheme for PV systems operating under partially shaded conditions," in International Conference on Advances in Green Energy (ICAGE), 17–18 December 2014 (Thiruvananthapuram, India: IEEE). doi:10.1109/icage.2014.7050141

Subudhi, B., and Pradhan, R. (2013). A comparative study on maximum power point tracking techniques for photovoltaic power systems. *IEEE Trans. Sustain. Energy* 4 (1), 89–98. doi:10.1109/tste.2012.2202294

Tamrakar, V., Sawle, S. C. Y., and Sawle, Y. (2015). "Study of characteristics of single and double diode electrical equivalent circuit models of solar PV module," in 2015 International Conference on Energy Systems and Applications, 30 October 2015 - 01 November 2015 (Pune, India: IEEE), 312–317. doi:10.1109/ICESA.2015.7503362

Thentral, T. M. T., Palanisamy, R., Usha, S., Bajaj, M., Zawbaa, H. M., Kamel, S., et al. (2022). Analysis of Power Quality issues of different types of household applications. *Energy Rep.* 8, 5370–5386. doi:10.1016/j.egyr.2022.04.010

Tsai, H., Tu, C., and Su, Y. (2008). "Development of generalized photovoltaic model using MATLAB/SIMULINK," in Proceedings of the World Congress on Engineering and Computer Science, 22–24 October, 2008 (San Francisco: IEEE).